

---

## Quality monitoring of a closed-loop system with parametric uncertainties and external disturbances: a fault detection and isolation approach

---

M. A. Rahim<sup>1</sup> · Haris M. Khalid<sup>2</sup> · Muhammad Akram<sup>2</sup> · L. Cheded<sup>2</sup> · Rajamani Doraiswami<sup>3</sup> · Amar Khoukhi<sup>2</sup>

<sup>1</sup>*Faculty of Business Administration, University of New Brunswick, Fredericton, E3B 5A3, Canada*

<sup>2</sup>*Department of Systems Engineering, King Fahd University of Petroleum and Minerals, Dhahran 31261, Saudi Arabia*

<sup>3</sup>*Department of Electrical and Computer Engineering, University of New Brunswick, Fredericton, E3B 5A3, Canada*

Correspondence should be addressed to Haris M. Khalid, mhariskh@kfupm.edu.sa

**Abstract** Due to aging and environmental factors, system components may either fail or not function as expected, which causes unprecedented changes in the quality of the system. A timely detection of the onset of a fault in a component is crucial to a quality monitoring of a process if costly failures are to be avoided. However, finding the source of the failure is not trivial in systems with a large number of components and complex component relationships. In this paper, an efficient scheme to detect adverse changes in system reliability and find the failed component is proposed in order to have an effective process quality monitoring. The monitoring scheme has been made effective by implementing first the techniques of fixed-parameter Shewhart, MEWMA and Hotelling's  $T^2$  control chart, and then the adaptive versions of Shewhart Chart, MEWMA and  $T^2$  control chart for counter-checking the precision of quality reports. Once detected, the fault isolation scheme uses a Bayesian decision strategy based on the maximum correlation between the residual and one of a number of hypothesized residual estimates to generate a fault report. By doing so, the critical information about the presence or absence of a fault, and its isolation, is gained in a timely manner, thus making the quality monitoring system an effective tool for a variety of maintenance programs, especially of the preventive type. The proposed scheme is evaluated extensively on simulated examples, and on a physical fluid system exemplified by a benchmarked laboratory-scale two-tank system to detect and isolate faults including sensor, actuator and leakage ones.

**Keywords** Quality monitoring · Fault detection · Adaptive Shewhart chart · Adaptive EWMA · Adaptive  $T^2$  chart · Benchmarked laboratory-scaled two tank system

**Biographical notes:** M. A. Rahim is a Professor of Quantitative Methods in the Faculty of Business Administration, University of New Brunswick, Fredericton, Canada. He received his Ph.D. in Industrial Engineering from the University of Windsor, M.Sc. in Systems Theory from the University of Ottawa, D.S. in Operations Research from the University of Rome, and M.Sc. in Statistics from the University of Dhaka. His research interests are in statistical process control, inventory control, maintenance policy and Total Quality Management. He serves on the editorial boards of several international journals.

Haris M. Khalid is a Ph.D. Student in the Department of Systems Engineering, King Fahd University of Petroleum and Minerals (KFUPM), Dhahran, Saudi Arabia. He is involved in the research projects of identification and performance monitoring of industrial based prototype systems, stabilization and control of critical non-linear systems.

Muhammad Akram is an M.S. Student in the Department of Systems Engineering, King Fahd University of Petroleum and Minerals (KFUPM), Dhahran, Saudi Arabia.

L. Cheded (St. M'81, M'88, SM'2003) gained his Ph.D. in Signal Processing from the University of Manchester (ex-UMIST), UK, in 1988. While at UMIST, he taught Physics to first-year students at the textile technology department (1980-1981) and was a teaching and research assistant at the Department of Instrumentation and Analytical Science (DIAS) during the period 1981-1984. He has been with the Systems Engineering department of the King Fahd University of Petroleum and Minerals in the Kingdom of Saudi Arabia (KSA) since September 1984, where he is currently an Associate Professor. He is currently a Senior Member of the IEEE, a member of the IET and a past member of EURASIP. He served as a member of the editorial board of the International Journal of Electrical Engineering Education during the period 1994-2005. His research interests are in signal processing, estimation and control, including fault diagnosis using various tools.

Rajamani Doraiswami ( M'76-SM '85) obtained his B.E. from Victoria Jubilee Technical Institute, Bombay, India, M.E. from the Indian Institute of Science, Bangalore, India and Ph.D from Johns Hopkins University, Baltimore, USA all in Electrical Engineering, in 1962, 1965 and 1971, respectively. He was a professor of Electrical Engineering at the Federal University of Santa Catarina, Florianopolis, Santa Catarina, Brazil from 1971 to 1981, and at the Federal University of Rio de Janeiro, Rio de Janeiro,

Brazil from 1976-1978. From 1981-2006 he has been with the University of New Brunswick, Fredericton, New Brunswick, Canada as professor of electrical and computer engineering. Since 2007, he is a professor emeritus at the University of New Brunswick. He is a senior member of the IEEE, fellow of the Indian Institute of Engineers and a Professional Engineer in the province of New Brunswick, Canada.

Amar Khoukhi is an Assistant Professor of Systems Engineering, KFUPM, Dhahran, Saudi Arabia. His area of research includes robotics and artificial intelligence, soft computing and fault diagnosis.

---

## 1 Introduction

The problem of monitoring the quality of a plant has always been recognized as being of primary importance and has been the subject of intense research for quality engineers. Diagnosis of unprecedented changes in system reliability and detection of the source of the change is essential for removing faulty components, replacing them with better ones, restructuring system architecture, and thus improving the overall system reliability. However, modern complex systems create challenges for systems engineers to understand and trouble-shoot possible system problems. Therefore due to the large system size, the use of efficient monitoring and fault diagnosis methods become unavoidable for complex systems [1].

Measurements are needed to monitor process efficiency and equipment condition. Data from a faulty component is composed of a time series of measurements of all the state variables describing this component.

For example, in the case of a simulated leak, the leak flow is initially set to zero for the first element of the series, and its value is gradually increased with time.

A single excursion of a component out of its limits is not enough to detect safely the presence of a fault in the process. An error is only flagged when a component remains out of bounds during several consecutive steps.

Monitoring is a continuous real-time task of determining the conditions in a physical system. It consists of recording information, recognizing changes and detecting abnormalities in the system's behavior. The faults to be monitored that are considered here include sensor, actuator and leakage faults, and can be classified broadly as either parametric faults or additive ones. An additive fault manifests itself as an additive exogenous signal in the measured data, while a parametric one induces a variation in the system parameters.

## 2 Related works

Related studies conducted in this area consist of three categories: quality monitoring models, statistical process control tools and both univariate and multivariate approaches to monitoring.

### 2.1 Quality monitoring

Various hydraulic models have been proposed to detect leaks in water distribution systems. Minimizing the difference between measured and calculated pressure and flow gives the solution to an inverse problem [2].

Liggett and Chen [3] extended this method to transient flow. These approaches can detect network leakage at nodal points only and require large amounts of data. Liou and Tian [4] developed a time marching algorithm to detect small and moderate size leaks under both steady and transient flow conditions. In the impulse response method, Liou [5] involves cross correlations between low amplitude pseudo random binary disturbance input and systems output. One or more leaks can be detected and located by the impulse response method. Mpesha et al. [6-7] applied a frequency response method using a step excitation to detect and locate leaks. Statistical methods for detecting leakage rates include a variety of approaches such as: the generalized likelihood ratio test in Mukherjee and Narasimhan [8], stratified random sampling with leak flow gauging in Arreguín-Cortes and Ochoa-Alejo [9], and standard weighted least squares state-estimation in Andersen and Powell [10]. Of the leak detection methods mentioned above, it is noteworthy that only one has actually been tested in the field.

Quality monitoring of production systems includes observation of the product quality, process quality and functioning of machines. Also the reporting can be considered as a monitoring method. Information about process conditions and quality data enables the analysis and implementation of process and quality control mechanisms. In the following sections, a general framework for monitoring of a real-time closed loop process control system is presented.

### 2.2 Statistical process control tools

The authors of [11] used Multivariate statistical process control MSPC to an electrolysis process. They also showed that the univariate analysis gives confusing results with regards to outlier detection, while the multivariate approach identifies two types of outliers. The study in [12] describes the development of Multivariate Statistical Process Control (MSPC) procedures for monitoring batch processes and demonstrates its application with respect to industrial tylosin biosynthesis. In [13], the authors

analyze multivariate statistical techniques for identifying and isolating abnormal process behavior. These techniques include contribution charts and variable reconstructions that relate to the application of principal component analysis (PCA). In [14], the author has implemented different multivariate statistical approaches for analyzing wastewater treatment process data and compared them with each other. In [15], the multi-scale principal component analysis (MSPCA) is used for fault detection and diagnosis.

### 2.3 Multivariate and univariate approaches to quality monitoring

Conventional, well-established statistical process monitoring charts, such as Shewhart, CUSUM (cumulative sum) charts [16] are of a univariate nature. These charts commonly only permit investigation into the magnitude of the deviation of any one variable, independently of all other variables, at a given time, often resulting in inaccurate, delayed conclusions being drawn [17].

Recently multivariate CUSUM and multivariate EWMA schemes [18][19] have been proposed and shown better and more powerful than  $T^2$  control chart particularly for small or moderate process shifts. In order to increase the power of the original  $T^2$  control chart, Grigoryan [20] proposed the multivariate multiple sampling (MMS) control chart scheme, which is a multivariate extension of a double sampling (DS) X chart with at least two sampling stages. The assumption of MMS or DS charts is that the minimum time between successive samples is negligible. The DS X chart was proposed by Daudin [21] to improve the statistical efficiency of the X chart without increasing the sampling. Daudin’s work has also been successfully extended to the monitoring of process variability [22] as well as the joint monitoring of process mean and variability [23].

The main contributions of this paper is the integration of various fixed and adaptive techniques for quality monitoring and the Bayesian inference system for fault isolation to achieve both accuracy and reliability of Quality Monitoring Scheme. This paper is organized as follows: Section 1 gives the Introduction, Section 2 describes comprehensively the related work done in quality monitoring. The problem statement for quality monitoring and fault detection is presented in Section 3. Section 4 gives the implementation and results of the proposed scheme. Section 5 discusses the criteria to assess early warning detection and finally some conclusions are given Section 6.

### 3 The quality monitoring and fault detection problem statement

Fault is an undesirable factor in any process control industry. It affects the efficiency of the system operation and reduces the economic benefit to the industry. The early detection and diagnosis of faults in mission critical systems becomes highly crucial for preventing failure of equipment, loss of productivity and profits, management of assets, reduction of shutdowns.

To have an effective plan for fault detection and analysis, a quality monitoring approach is employed so as to meet the requirements for a quick and reliable fault detection and isolation scheme and thus ensuring a sound quality monitoring program. The proposed scheme has been evaluated on a process control system. Quality monitoring and fault detection are carried out by jointly interpreting model outputs. The implementation plan for the proposed scheme is as shown in Figure 1. It should be noted that a fault report is also considered as part of the Quality monitoring of the system. The proposed scheme has been evaluated on a benchmarked laboratory scale two-tank apparatus. It is the most used prototype applied in wastewater treatment,–petrochemical, and oil/gas plants. The evaluation of the proposed scheme is done by considering the following structured diagram.

#### 3.1 System description

The benchmarked laboratory-scale process control system has been used to collect data. The data has been collected at a sampling time of 50 millisecond. The different data sets have been generated for a PI-Controlled water level control. Different fault scenarios have also been considered for the generation of the data sets.

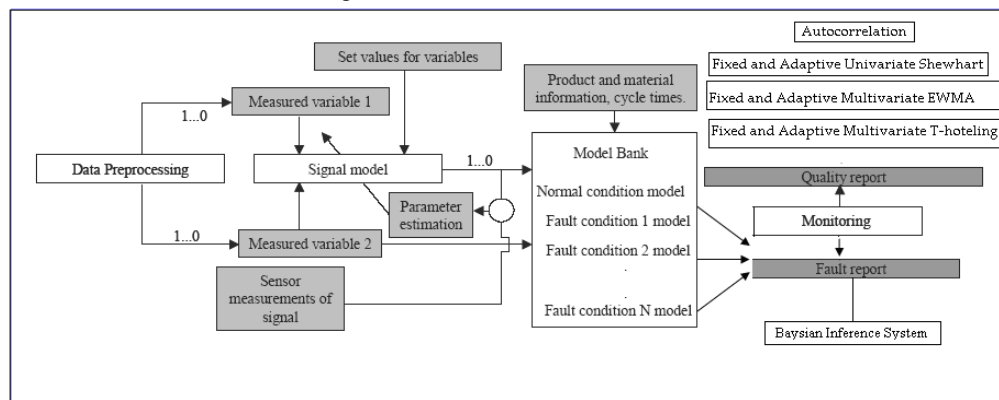


Figure 1: Implementation plan for the evaluation of the proposed scheme

### 3.2 Experimental setup

The process Data has been generated through an experimental setup as shown in Figure 2. A two-tank system has been used in order to collect the data with the introduction of actuator and sensor faults through the system as can be seen in the labview circuit window. An amplified voltage of 18 volts has been used to handle the controller effectively for the changes/fluctuation produced in the system. So, the fault diagnosis was done here in a closed-loop set-up where the controller is actually trying to suppress the faults as though they were disturbances.

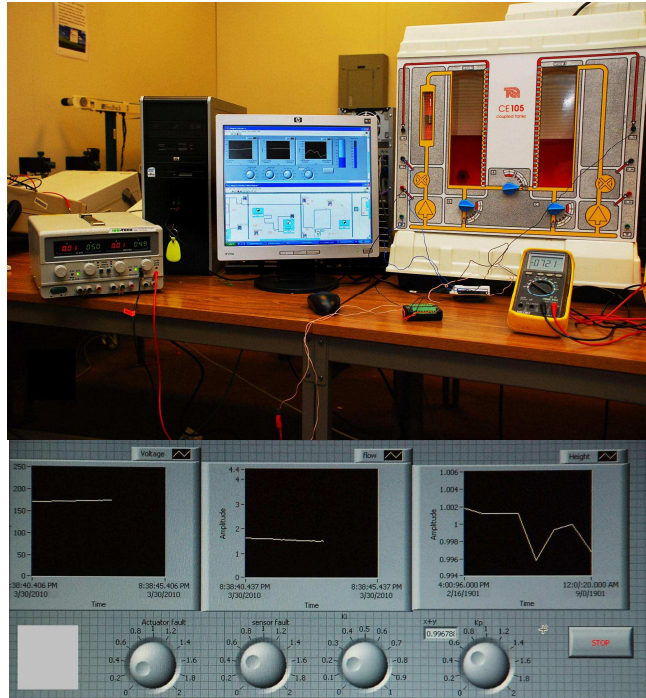


Figure 2 A – The two tank system interfaced with the Labview through a DAQ and the amplifier for the magnified voltage , B – The labview setup of the apparatus including the circuit window and the block diagram of the experiment.

### 3.3 Process data collection and description

The process data has been collected at 50 millisecond- sampling time. The main objective of the benchmarked dual-tank system is to reach a reference height of 200 ml of the second tank. During this process, several faults have been introduced such as the leakage faults, sensor faults and actuator faults. The leakage faults have been introduced through the pipe clogs of the system, knobs between the first and the second tank, etc. The sensor faults have been simulated by introducing a gain in the circuit as if there is a fault in the level sensor of the tank. Similarly, the actuator faults have been simulated by introducing a gain in the setup for the actuator that comprises of the motor and pump. A PI controller has been employed in order to reach the desired reference height. Due to the inclusion of faults, the controller was finding it difficult to reach the desired level. For this reason, the power of the motor has been increased from 5 volts to 18 volts in order to provide it with the maximum throttle to reach the desired level. This enabled the actuator to perform well in achieving its desired level but led to the controller suppressing the faults injected into the system. So, this made the fault detection task rather difficult. After the data collection task was completed, techniques such as settling time, steady-state value, and coherence spectra were used to help us get an insight into the faults present in the system.

### 3.4 Model of the coupled tank system

The physical system under evaluation is formed of two tanks connected by a pipe. The leakage is simulated in the tank by opening the drain valve. A DC motor-driven pump supplies the fluid to the first tank and a PI controller is used to control the fluid level in the second tank by maintaining the level at a specified level, as shown in Fig. 2.

A step input is applied to the dc motor- pump system to fill the first tank. The opening of the drainage valve faults introduces a leakage in the tank. Various types of leakage are introduced and the liquid height in the second tank,  $H_2$ , and the inflow rate,  $Q_i$ , are both measured. The National Instruments LABVIEW package is employed to collect these data.

A benchmark model of a cascade connection of a dc motor and a pump relating the input to the motor,  $u$ , and the flow,  $Q_i$ , is a first-order system:

$$\dot{Q}_i = -a_m Q_i + b_m \phi(u) \quad (1)$$

where  $a_m$  and  $b_m$  are the parameters of the motor-pump system and  $\phi(u)$  is a dead-band and saturation type of nonlinearity. It is assumed that the leakage  $Q_l$  occurs in tank 1 and is given by:

$$Q_l = C_{dl} \sqrt{2gH_1} \quad (2)$$

With the inclusion of the leakage, the liquid level system is modeled by:

$$A_1 \frac{dH_1}{dt} = Q_i - C_{12} \phi(H_1 - H_2) - C_l \phi(H_1) \quad (3)$$

$$A_2 \frac{dH_2}{dt} = C_{12} \phi(H_1 - H_2) - C_o \phi(H_2) \quad (4)$$

where  $\phi(\cdot) = \text{sign}(\cdot) \sqrt{2g(\cdot)}$ ,  $Q_l = C_l \phi(H_1)$  is the leakage flow rate,  $Q_o = C_o \phi(H_2)$  is the output flow rate,  $H_1$  is the height of the liquid in tank 1,  $H_2$  is the height of the liquid in tank 2,  $A_1$  and  $A_2$  are the cross-sectional areas of the 2 tanks,  $g=980 \text{ cm/sec}^2$  is the gravitational constant,  $C_{12}$  and  $C_o$  are the discharge coefficient of the inter-tank and output valves, respectively.

The model of the two-tank fluid control system, shown above in Fig. 3, is of a second order and is nonlinear with a smooth square-root type of nonlinearity. For design purposes, a linearized model of the fluid system is required and is given below in (5) and (6):

$$\frac{dh_1}{dt} = b_1 q_i - (a_1 + \alpha) h_1 + a_1 h_2 \quad (5)$$

$$\frac{dh_2}{dt} = a_2 h_1 - (a_2 - \beta) h_2 \quad (6)$$

where  $h_1$  and  $h_2$  are the increments in the nominal (leakage-free) heights  $H_1^0$  and  $H_2^0$ :

$$b_1 = \frac{1}{A_1}, \quad a_1 = \frac{C_{db}}{2\sqrt{2g(H_1^0 - H_2^0)}}, \quad \beta = \frac{C_o}{2\sqrt{2gH_2^0}}, \quad a_2 = a_1 + \frac{C_{do}}{2\sqrt{2gH_2^0}}, \quad \alpha = \frac{C_{dl}}{2\sqrt{2gH_1^0}}$$

and the parameter  $\alpha$  indicates the amount of leakage.

A PI controller, with gains  $k_p$  and  $k_i$ , is used to maintain the level of the Tank 2 at the desired reference input  $r$ .

where  $q_i, q_l, q_o, h_1$  and  $h_2$  are the increments in  $Q_i, Q_l, Q_o, H_1^0$  and  $H_2^0$ , respectively, the parameters  $a_1$  and  $a_2$  are associated with linearization whereas the parameters  $\alpha$  and  $\beta$  are respectively associated with the leakage and the output flow rate, i.e.  $q_l = \alpha h_1$ ,  $q_o = \beta h_2$ .

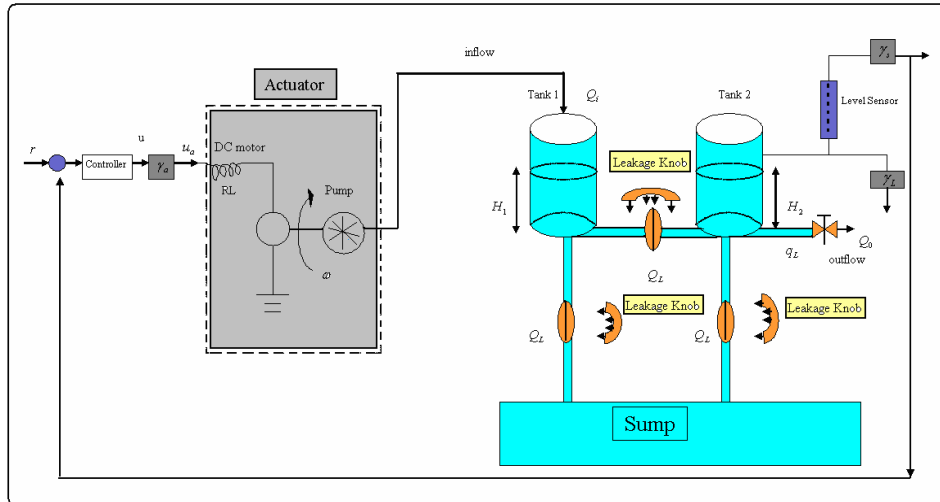


Figure 3. Two-tank model

## 4 Implementation and simulation results

### 4.1 Analysis of fixed and adaptive Shewhart chart

An analysis of the fixed and adaptive shewhart control chart is carried out here and which has been thoroughly tested through extensive simulation runs and also through an evaluation on the physical system. As mentioned earlier, various types of leakage faults were introduced by opening the drainage valve and the liquid height profiles in the second tank were subsequently

analyzed. Also, the actuator and sensor faults were also introduced. The univariate adaptive Shewhart algorithm can be described as follows:

4.2 Adaptive Shewhart algorithm:

*Step I:* Select a number of samples  $n$ , Great mean of input variable  $height \bar{X}_1$ , Great mean of input variable  $flow \bar{X}_2$ , Standard Deviation of height  $S_{height}$ , Standard Deviation of flow  $S_{flow}$  which is plotted on a chart.

*Step II:* Determine Upper Control Limit (UCL) of the chart,  $UCL=(sum(flow/height,1)/N)+((3*s)/sqrt(N))$ ; (9)  
Where  $s$  is the standard deviation of the flow/height and  $N$  is the number of samples.

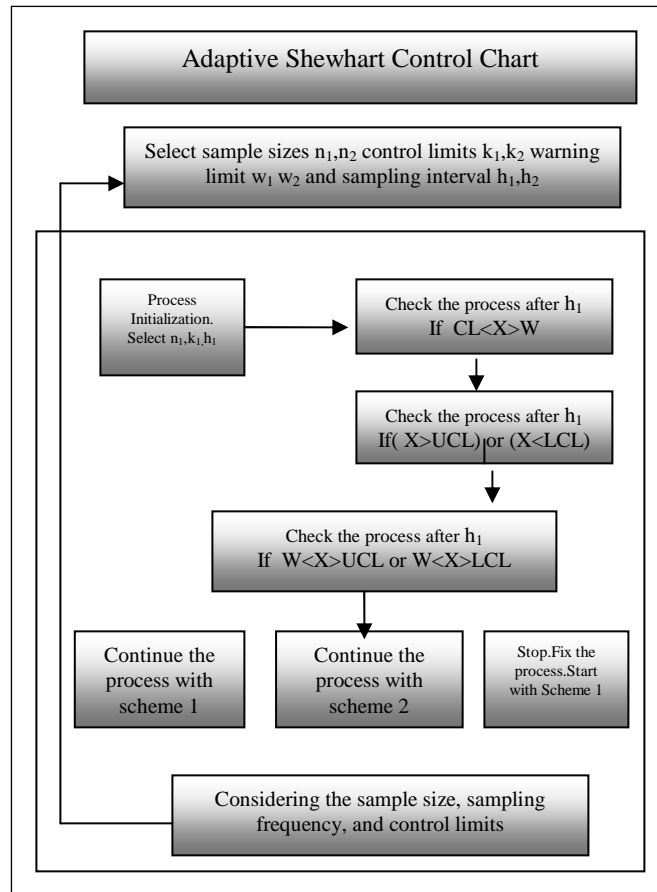


Figure 4. Flow Chart for adaptive Shewhart

*Step III:* Determine Lower Control Limit (LCL) of the chart,  $LCL=(sum(flow/height,1)/N)-((3*s)/sqrt(N))$ ; (10)

Where  $s$  is the standard deviation of the flow/height and  $N$  is the number of samples.

*Step IV:* Considering the following sampling time for all the cases:

Sampling time\_usual=10;

Sampling time\_upper control limit=5;

Sampling time\_lower control limit=5;

*Step V:* Now while everything is usual, the usual sampling time is applied. If  $flow/height > UCL$ , then sampling time=sampling time\_upper control limit, Else sampling time=sampling time\_usual. If  $flow/height < LCL$ , then sampling time=sampling time\_lower control limit, Else sampling time=sampling time\_usual.

*Note:* It should be noted that the parameters which have been made adaptive here are the sample size, sampling frequency and the UCL/LCL control limits to capture the fault effectively.

A general flow chart for the implementation of the Adaptive shewhart algorithm is as shown in Fig. 4.

It has been found that both fixed and adaptive versions performed well for medium and high levels of leakage, sensor and actuator faults as shown in Table I and Fig. 5-8 for both flow and height profiles. However, the Shewhart scheme was unable to

detect incipient faults. Also, as there are two variables to be measured, so fixed and adaptive versions of shewhart were not found to be consistent in showing the same results for both input variables to be measured.

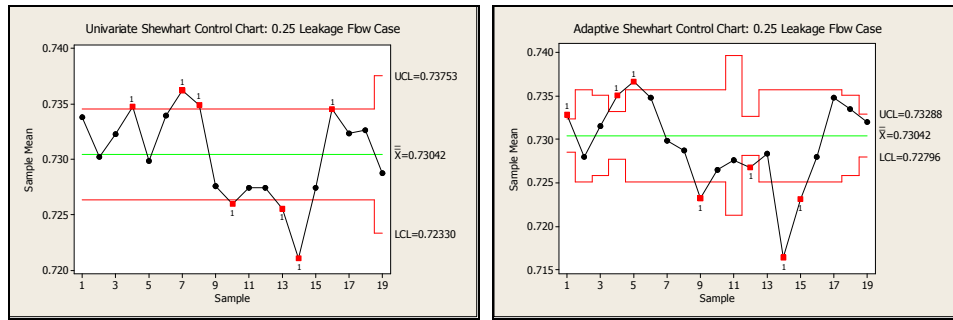


Figure 5 (a) Univariate Shewhart Control Chart: 0.50 Leakage Flow Case (b) Adaptive Shewhart Control Chart: 0.50 Leakage Flow Case

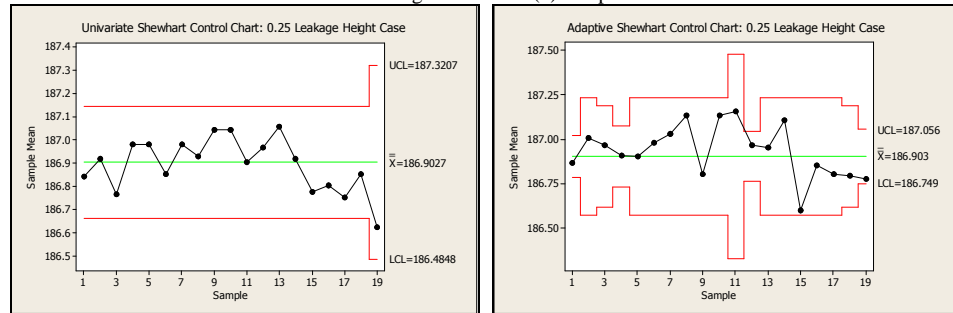


Figure 6 (a) Univariate Shewhart Control Chart: 0.50 Leakage Height Case (b) Adaptive Shewhart Control Chart: 0.50 Leakage Height Case

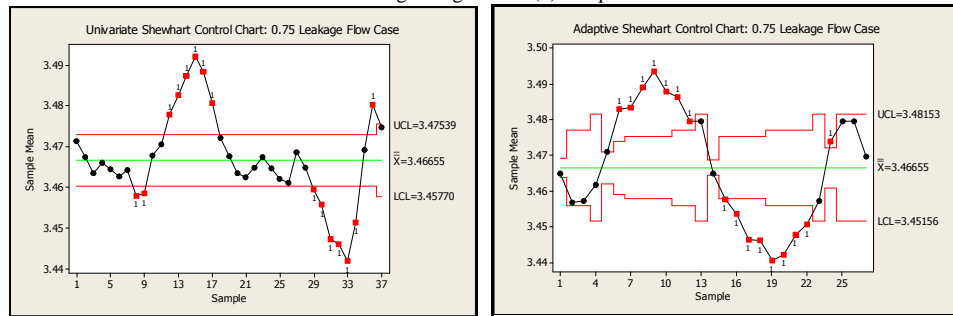


Figure 7 (a) Univariate Shewhart Control Chart: 0.75 Leakage Flow Case (b) Adaptive Shewhart Control Chart: 0.75 Leakage Flow Case

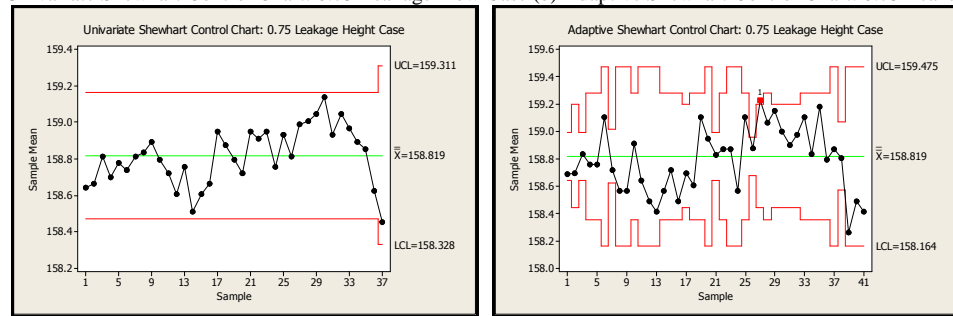


Figure 8 (a) Univariate Shewhart Control Chart: 0.75 Leakage Height Case (b) Adaptive Shewhart Control Chart: 0.75 Leakage Height Case

### 4.3 Analysis of fixed and adaptive MEWMA chart

An analysis of fixed and adaptive EWMA control chart is carried out here and which has been thoroughly tested through extensive simulation runs and also through an evaluation on the physical system. As mentioned earlier, various types of leakage faults were introduced by opening the drainage valve and the liquid height profiles in the second tank were subsequently analyzed. Also, the actuator and sensor faults have also been introduced in this experiment. The multivariate EWMA algorithm is as follows:

#### 4.2.1 Multivariate exponentially weighted moving-average (MEWMA) algorithm:

Step I: Find  $z_i$  corresponding to each sample value.

$$z_i = \lambda x_i + (1 - \lambda)z_0 \tag{11}$$

Where  $\lambda$  is the weighting parameter

$x_i$  is the sample value with  $i = 1, 2, 3, \dots, n$

$z_0 = \bar{x}$  is the sample mean, and

$\lambda, 0 \leq \lambda \leq 1$

Also,  $T_i^2 = z_i' \Sigma^{-1} z_i$  where  $T_i^2$  determines the auto-correlation.

Step II: Compute UCL and LCL for each period I of multi-variate.

$$\text{Step III: } UCL = \mu_0 + L\sigma \sqrt{\frac{\lambda}{(2-\lambda)}} [1 - (1-\lambda)^{2i}] \tag{12}$$

Centerline =  $\mu_0$

$$LCL = \mu_0 - L\sigma \sqrt{\frac{\lambda}{(2-\lambda)}} [1 - (1-\lambda)^{2i}] \tag{13}$$

Where  $L$  is the width of control limit,  $\sigma$  is the standard deviation.

Step IV: Now while everything is usual, the usual sampling time is applied. If  $\text{flow/height} > UCL$ , then  $\text{sampling time} = \text{sampling time\_upper control limit}$ , Else  $\text{sampling time} = \text{sampling time\_usual}$ . If  $\text{flow/height} < LCL$ , then  $\text{sampling time} = \text{sampling time\_lower control limit}$ , Else  $\text{sampling time} = \text{sampling time\_usual}$ .

Note: It should be noted that the parameters which have been made adaptive here are the sample size, sampling frequency and the UCL/LCL control limits to capture the fault effectively.

It has been found that both fixed and adaptive versions performed well for all levels of leakage, sensor and actuator faults as shown in Table II (Same remark as above and Figures 9-11. For both input variables to be measured, the results are found to be very reliable. This scheme has the ability to capture the input-output dynamic behavior, and not the dynamics resulting from the effect of noise and other artifacts.

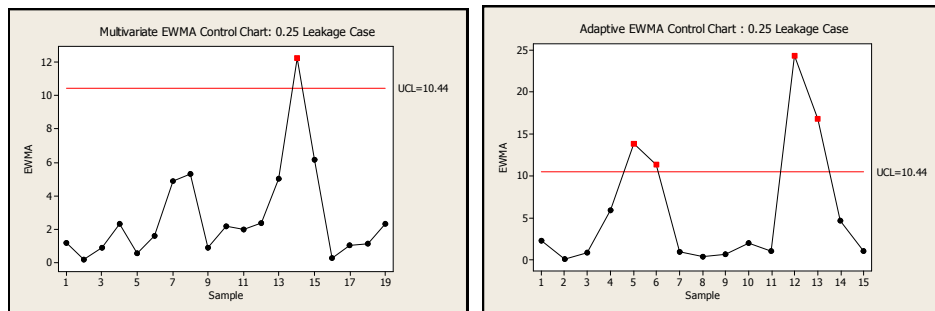


Figure 9 (a) Multivariate EWMA Control Chart: 0.25 Leakage Fault Case (b) Adaptive EWMA Control Chart: 0.25 Leakage Fault Case

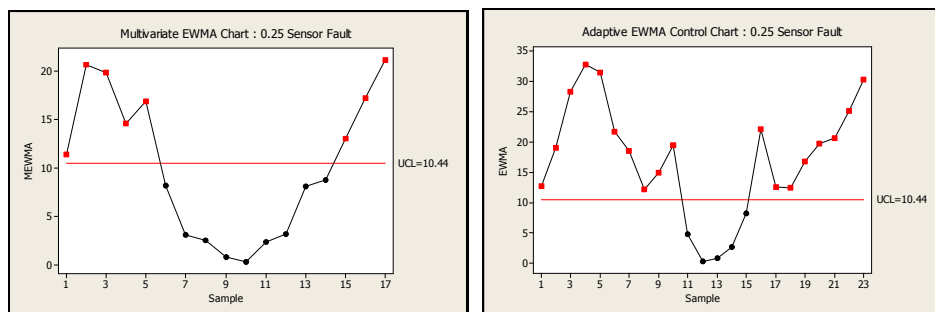


Figure 10 (a) Multivariate EWMA Control Chart: 0.25 Sensor Fault Case (b) Adaptive EWMA Control Chart: 0.25 Sensor Fault Case



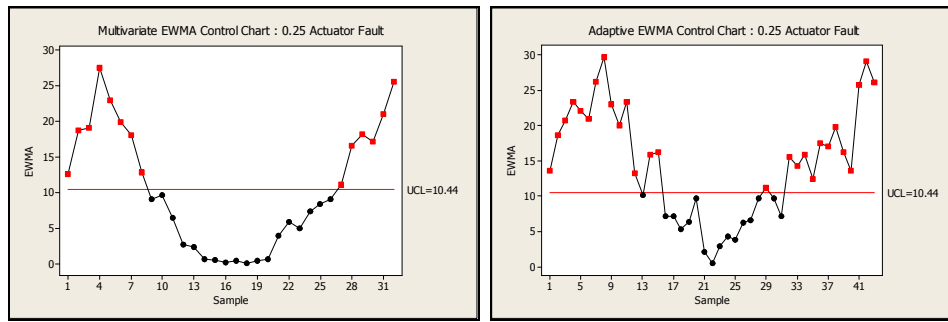


Figure 11 (a) Multivariate EWMA Control Chart: 0.25 Actuator Fault Case (b) Adaptive EWMA Control Chart: 0.25 Actuator Fault Case

#### 4.4 Analysis of fixed and adaptive $T^2$ chart

Here the analysis of fixed and adaptive  $T^2$  control chart is carried out and thoroughly tested through extensive simulation runs and an also through an evaluation on the physical system. As mentioned earlier, various types of leakage faults were introduced by opening the drainage valve and the liquid height profiles in the second tank were subsequently analyzed. Also, the actuator and sensor faults are being introduced.

##### 4.4.1 Multivariate $T^2$ Hotelling algorithm:

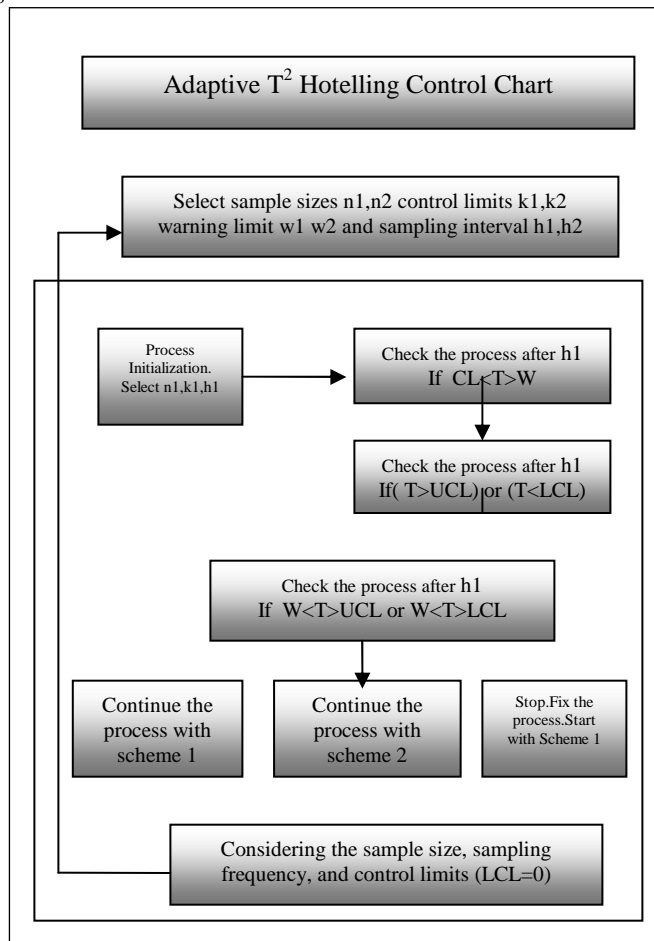


Figure 12. Flow Chart for adaptive  $T^2$  Algorithm

*Step I:* Select a number of samples  $n$ , Great mean of input variable  $height \bar{X}_1$ , Great mean of input variable  $flow \bar{X}_2$ , Square of Standard Deviation of height  $S^2_{height}$ , Standard Deviation of flow  $S^2_{flow}$ . And Standard Deviation of both  $height$  and  $flow$  as  $S_{flow/height}$ . The test statistics is given by:

$$T^2 = n(\bar{X} - \bar{\bar{X}})' S^{-1} (\bar{X} - \bar{\bar{X}}) \quad (14)$$

And is plotted on the chart (Fig 10-12)

Step II: Select  $UCL = \frac{p(m-1)(n-1)}{mn-m-p+1} F_{\alpha,p,mn-m-p+1}$  (15)

where  $p$  is the quality characteristics for the flow and height,  $m$  are the number of samples taken for flow and height,  $n$  is the sample size i.e. 2 as we have two input variables i.e. flow ad height.

$F_{\alpha,p,mn-m-p+1}$  is the degree of freedom.

Step III: Select LCL=0

Step IV:

Considering the following sampling time for all the cases:

Sampling time\_usual=10;

Sampling time\_upper control limit=5;

Sampling time\_lower control limit=5;

Step V: Now while everything is usual, the usual sampling time is applied. If flow/height>UCL, then sampling time=sampling time\_upper control limit, Else sampling time=sampling time\_usual. If flow/height<LCL, then sampling time=sampling time\_lower control limit, Else sampling time=sampling time\_usual.

Note: It should be noted that the things which have been made adaptive here are the sample size, sampling frequency and the UCL/LCL=0 control limits to capture the fault effectively.

A general flow chart for the implementation of the Adaptive T<sup>2</sup> algorithm is shown in Fig. 12.

It has been found that both fixed and adaptive versions performed well for all levels of leakage, sensor and actuator faults as shown in Table III and Figures 13-15. For both input variables to be measured, the results are found to be very reliable. This scheme has the ability to capture the input-output dynamic behavior, and the dynamics resulting from the effect of noise and other artifacts.

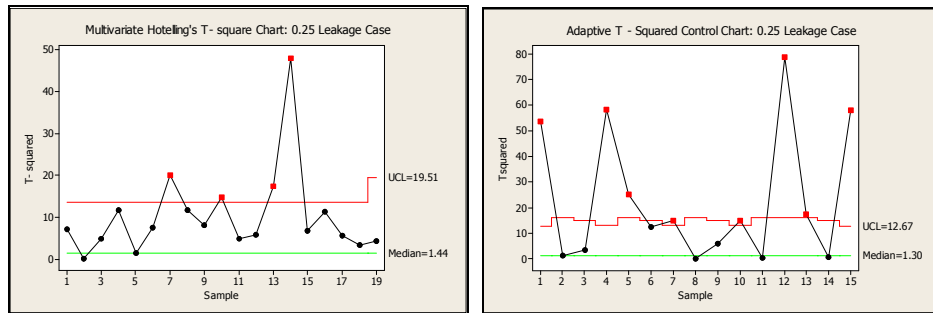


Figure 13 (a) Multivariate T<sup>2</sup> Control Chart: 0.25 Leakage Fault Case (b) Adaptive T<sup>2</sup> Control Chart: 0.25 Leakage Fault Case

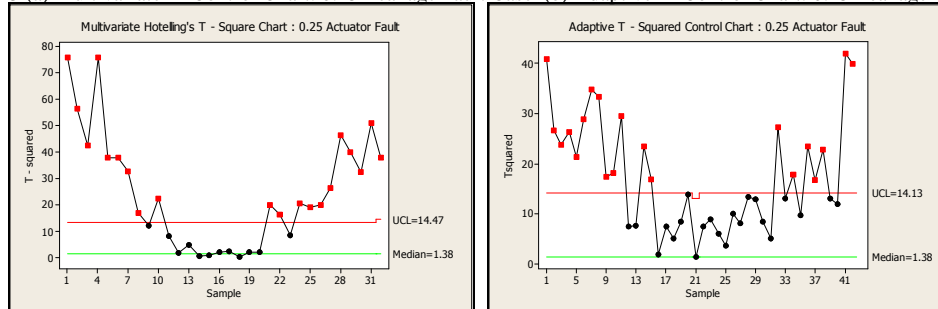


Figure 14 (a) Multivariate T<sup>2</sup> Control Chart: 0.25 Actuator Fault Case (b) Adaptive T<sup>2</sup> Control Chart: 0.25 Actuator Fault Case

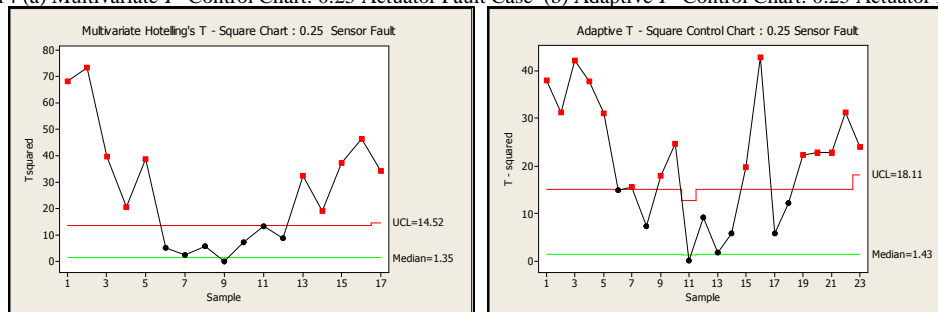


Figure 15 (a) Multivariate T<sup>2</sup> Control Chart: 0.25 Actuator Fault Case (b) Adaptive T<sup>2</sup> Control Chart: 0.25 Actuator Fault Case

## 4.5 Analysis of Bayesian inference system for fault detection

A statistical decision-theoretic approach was used to decide between two hypotheses. If the absolute value of the mean of the residual is less than a specified threshold value,  $thr$ , then a fault is asserted. The threshold value is calculated from the pre-specified false alarm rate, and the variance of the residual.

The approach, employed here is based on a isolation model, which relates directly the detection parameters to the input and output, and which is identified offline by performing a number of experiments. The detection model relating the reference input,  $r$ , the detection parameter,  $\gamma$  and the residual  $e(k)$ , is given by:

$$e(k) = y(k) - y^0(k) = \sum_{i=1}^q \psi^T(k-1) \theta_i^{(1)} \Delta \gamma_i + v(k) \quad (16)$$

where,  $\Delta \gamma_i = \gamma - \gamma_i^0$  is the perturbation in  $\gamma$ ;  $y^0(k)$  and  $\gamma_i^0$  are the fault-free (nominal) output and parameter respectively,  $\theta_i^{(1)} = \frac{\delta \theta}{\delta \gamma_i}$ , and  $\psi$  is the data vector formed of the past outputs and past reference inputs. The gradient  $\theta_i^{(1)}$ , is estimated by performing a number of offline experiments which consist of perturbing the detection parameters, one at a time. The input-output data from all the perturbed parameter experiments is then used to identify the gradients  $\theta_i^{(1)}$ . The hypothesis,  $H_i$  corresponding to the perturbation of the  $i^{\text{th}}$  detection parameter is given by:

$$H_i : e(k) = \psi^T(k-1) \theta_i^{(1)} \Delta \gamma_i + v(k) \quad (17)$$

If  $v(k)$  is a zero-mean Gaussian random variable, then the Bayes strategy suggests that the *most likely* hypothesis,  $H_j$  is the one that satisfies,

$$j = \arg \min_i \left\{ \left\| e(k) - \psi^T(k-1) \theta_i^{(1)} \Delta \gamma_i \right\|^2 \right\} \quad (18)$$

Since the size of the fault, denoted by the perturbation  $\Delta \gamma_j(k)$ , is unknown, a composite hypothesis testing scheme is used in which we substitute the unknown  $\Delta \gamma_j(k)$  by its least-squares estimate. Substituting the estimate of  $\Delta \gamma_j(k)$  and simplifying the fault isolation strategy yields:

$$j = \arg \max_i \left\{ \cos^2 \varphi_i \right\} \quad \text{where} \quad \cos \varphi_i = \frac{\langle e, \psi^T \theta_i^{(1)} \rangle}{\|e\| \|\psi^T \theta_i^{(1)}\|} \quad (19)$$

That is,  $\gamma_j$  is asserted to be faulty if the measured residual,  $e(k)$ , and its hypothesized residual estimate,  $\psi^T(k-1) \theta_j^{(1)}$  are maximally aligned. A measure of isolability of faults in  $\gamma_i$  and  $\gamma_j$ , is defined by the cosine of the angle between  $\theta_i^{(1)}$  and  $\theta_j^{(1)}$ , denoted by  $\cos \theta_{ij}^{(1)}$ . The smaller  $\cos \theta_{ij}^{(1)}$  is, the larger the isolability gets.

The detection model of the fluid system becomes:

$$e(k) = \sum_{i=1}^3 \psi^T(k-1) \theta_i^{(1)} \Delta \gamma_i + v(k) \quad (20)$$

where  $\psi^T(k) = [-y(k-1) \quad -y(k-2) \quad u(k-1) \quad u(k-2)]$ ,

$\gamma_1 = \gamma_t$ ,  $\gamma_2 = \gamma_a$  and  $\gamma_3 = \gamma_s$

A number of experiments are performed offline by varying the detection parameters, one at a time. Each of the  $\gamma$  parameters was varied one at a time, spanning three different values of 0.25, 0.5 and 0.75 of their maximum, and from these experiments, the gradients  $\theta_i^{(1)}$  were estimated:

$$\theta^{(1)} = [\theta_t^{(1)} \quad \theta_a^{(1)} \quad \theta_s^{(1)}] = \begin{bmatrix} -0.2491 & 0.0042 & -0.2153 \\ 0.2456 & -0.0024 & 0.2169 \\ 1.0678 & 2.6411 & 4.0696 \\ -1.6474 & -2.1772 & -3.4557 \end{bmatrix} \quad (21)$$

The measure of isolability  $\cos \theta_{ij}^{(1)}$  is given below:

$$\cos \theta_{12}^{(1)} = 0.8560 \quad \cos \theta_{13}^{(1)} = 0.8379 \quad \cos \theta_{23}^{(1)} = 0.7757 \quad (22)$$

Using the composite hypothesis testing scheme, a fault is isolated by determining which hypothesis gives the maximal alignment of the estimated and the measured residuals. The results of the isolation scheme were encouraging.

## 5 Discussion on criteria to assess early warning detection

Online monitoring of alerting-system performance (e.g., true alarm and false alarm rates) based on alarm system (e.g. through estimating true alarm rates) depends on a number of parameters including, sensor accuracy, monitoring operation of instruments, thresholds, and human responses to an alert, Kuchar [24]. An early warning detection system algorithm is desirable. The following three criteria could be used to assess the efficacy of an early warning detection system/algorithm: (1) the probability of detection, (2) the probability of false alarm, and (3) the alarm time (i.e., time to detect a change).

Measurements involving errors can occasionally occur due to faults arising in the process. In particular, a system may fail to alert when necessary (which is termed a missed detection) or may issue an alert when one is not needed (which is termed a false alarm). Although both types of errors are undesirable, they cannot be eliminated simultaneously. Rather, some compromise between false alarms and missed detections is made through a judicious choice of the alerting threshold. For example, a conservative threshold results in an increase in early alerts, reducing the probability of missed detections, but increasing the probability of false alarms. If the threshold is adjusted to compensate, through a delay in issuing the alert signal until more information about the hazard becomes available, the false alarm rate will decrease, but the missed-detection rate will increase. A standard is fixed that provides the probability of detection at a determined minimum alarm level and the false alarm rate at a minimum alarm level. Performance standards for fault detectors often include requirements for the probability of a false alarm at a specified level of statistical confidence. One can choose a higher probability of detection, but with a higher false alarm rate, or choose a lower probability of detection and lower false alarm rate. Thus, the user is able to trade-off performance with detection probability, false alarm rate and cost.

In industrial management, a false alarm could refer either to an alarm with little informative content that can usually be safely detected or eliminated, or is triggered by a faulty instrument. In signal detection theory, a false alarm occurs where a non-target event exceeds the detection threshold. Signal-to-noise ratio is a measure used to quantify how much the signal has been disturbed or corrupted by noise. In quality control systems, two types of inspection errors are associated with using the control charts. These are Type I and Type II errors. Type I error is the result of concluding that the process is out-of-control, based on the actual data plotted on the chart, when it is actually in-control, thus signaling a false alarm. While the Type II error is the result of concluding that the process is in-control, based on the actual data plotted on the chart, when the process is out-of-control thus signaling a missed detection. The probability of Type I error is denoted by  $\alpha$  and the probability of Type II error is denoted by  $\beta$ .

The average run length (ARL) is another measure of the performance used to determine the time to detect a change. It is the number of samples required to detect an out-of-control state. It is measured as the reciprocal of the probability of a Type I error  $\alpha$ ,  $ARL = 1/\alpha$ . For a  $3\sigma$  control chart,  $ARL = 1/0.0026 = 385$ . This shows that on the average one sample point, out of 385, is expected to fall outside of the control limits, which is indicative of a high reliability of the system's operation.

## 6 Conclusion

In this paper, the complete process monitoring scheme was studied and it was shown that it can be made effective by implementing a variety of techniques, such as the fixed parameter Shewhart, MEWMA Hotelling's  $T^2$ , and the adaptive versions of Shewhart Chart, MEWMA and  $T^2$  Chart for providing quality reports and ensuring reliable fault detection. Moreover, the fault isolation report is provided through the use of the Bayesian Statistical Inference, thus completing the overall diagnostic picture of quality monitoring.

Two general approaches for the application of control charts were tested: fixed-, and variable-sampling interval approaches. When an adaptive sampling interval was used, then  $T^2$  Control Chart became more sensitive to the faults introduced into the system and outperformed EWMA, Hotelling's and the Shewhart techniques by reacting quicker to shifts in the process mean. As such, they can be used for a reliable detection of incipient faults, which in turn leads to an efficient and cost-effective preventive maintenance scheme.

The major contributions of the paper is the integration of various fixed and adaptive techniques for quality monitoring and the Bayesian inference system for fault isolation to achieve both accuracy and reliability of quality monitoring schemes. In future studies, comparisons with other techniques (as proposed in Ref. [18-22] would be worth investigating. A comparative study on various early warning fault detection criteria would also be an interesting area for further research.

### Acknowledgements

The authors acknowledge support provided by the National Science and Engineering Research Council (NSERC) and the Universities of KFUPM and UNB. The valuable suggestions and constructive criticisms of the two anonymous reviewers are gratefully acknowledged. We would also like to thank the editor of this journal for his guidance and efforts in improving the quality of this paper.

### References

1. Doguc O, Ramirez-Marquez JE (2009) An efficient fault diagnosis method for complex system reliability. In: 7th annual conference on systems engineering research (CSER 2009), Loughborough, UK
2. Pudar, RS, Ligget JA (1992) Leaks in pipe networks. *Journal of Hydraulic Engineering* 118(7):1031–1046
3. Ligget JA, Chen LC (1994) Inverse transient analysis in pipe networks. *Journal Hydraulic Engineering* 120(8):934–955
4. Liou, JCP, Tian J (1995) Leak detection-transient flow simulation approaches. *Journal of Energy Resource Technology* 117(3):243–248
5. Liou, CP (1998) Pipeline leak detection by impulse response extraction. *Journal of Fluids Engineering* 120(4):833–838
6. Mpesha W, Gassman SL, Chaudhry MH (2001) Leak detection in pipes by frequency response method. *Journal of Hydraulic Engineering* 127(2):134–147
7. Mpesha W, Gassman SL, Chaudhry MH (2002) Leak detection in pipes by frequency response method using a step excitation. *Journal of Hydraulic Research* 40(7):55–61
8. Mukherjee J, Narasimhan S (1996) Leak detection in networks of pipelines by generalized likelihood ratio method. *Industrial and Engineering Chemistry Journal* 35(6):1886–1893
9. Arreguín-Cortes FI, Ochoa-Alejo LH (1997) Evaluation of water losses in distribution networks. *Journal of Water Resource Planning Management* 123(5):284–291
10. Andersen JH, Powell RS (2000) Implicit state-estimation technique for water network monitoring. *Urban Water Journal* 2:123–130
11. Wikström C, Albano C, Eriksson L, Fridén H, Johansson E, Nordahl Å, Rännar S, Sandberg M, Kettaneh-Wold N, Wold S (1998) Multivariate process and quality monitoring applied to an electrolysis process. Part I. Process supervision with multivariate control charts. *Chemometrics and Intelligent Laboratory Systems* 42(1-2):221–231
12. Albert S, Kinley RD (2001) Multivariate statistical monitoring of batch processes: an industrial case study of fermentation supervision. *Trends in Biotechnology* 19(2):53–62
13. Lieftucht D, Kruger U, Irwin, GW (2006) Improved reliability in diagnosing faults using multivariate statistics. *Computers and Chemical Engineering* 30(5):901–912
14. Aguado D, Rosen C (2008) Multivariate statistical monitoring of continuous wastewater treatment plants. *Engineering Applications of Artificial Intelligence* 21(7):1080–1091
15. Misra M, Yu HH, Qin SJ, Ling C (2002) Multivariate process monitoring and fault diagnosis by multi-scale PCA. *Computers and Chemical Engineering* 26(9):1281–1293
16. Ogunnaike BA, Ray WH (1994) *Process dynamics, modelling, and control*. Oxford University Press, New York
17. Kourti T, MacGregor JF (1995) Process analysis, monitoring and diagnosis, using multivariate projection methods. *Chemometrics and Intelligent Laboratory Systems* 28(1):3–21
18. Crosier RB (1988) Multivariate generalizations of cumulative sum quality-control schemes. *Technometrics* 30:291–303
19. Lowry CA, Woodall WH, Champ CW, Rigdon SE (1992) A multivariate exponentially weighted moving average control chart. *Technometrics* 34:46–53
20. Grigoryan A, He D (2005) Multivariate double sampling S charts for controlling process variability. *International Journal of Production Research* 43(5):715–730
21. Daudin JJ (1992) Double sampling X-bar charts. *Journal of Quality Technology* 24(2):78–87
22. He D, Grigoryan A (2005) Multivariate multiple sampling charts. *IIE Transactions* 37(6):509–521
23. He D, Grigoryan A (2006) Statistical design of joint double sampling X and S charts. *European Journal of Operational Research* 168(1):122–142
24. Kuchar JT (1996) Methodology for alerting-system performance evaluation. *Journal of Guidance, Control, and Dynamics* 19(2):438–444

TABLE I.

TABLE II. ANALYSIS OF VARIOUS LEVELS OF LEAKAGE FAULTS, SENSOR FAULTS AND ACTUATOR FAULTS WITH FIXED AND ADAPTIVE SHEWHART CONTROL CHART

Univariate Shewhart Control Chart																									
		Process Parameters																							
		Fixed Parameters						Variable Parameters						Variable Parameters								Improvement (%)			
		Flow Variable			Height Variable			Flow Variable			Height Variable			Flow Variable				Height Variable				Error detection			
Cases	Subcase	Sample size n	Sampling Freq. h	Control limits k	Sample size n	Sampling Freq. h	Control limits k	n <sub>1</sub>	n <sub>2</sub>	h <sub>1</sub>	h <sub>2</sub>	k <sub>1</sub>	k <sub>2</sub>	w <sub>1</sub>	w <sub>2</sub>	n <sub>1</sub>	n <sub>2</sub>	h <sub>1</sub>	h <sub>2</sub>	k <sub>1</sub>	k <sub>2</sub>	w <sub>1</sub>	w <sub>2</sub>		
Case I: FAULTS <sub>Leakage</sub>	Subcase <sub>11</sub> (small)	4	1.2	3.45	4	1.2	3.45	4	9	1.2	1.0	3.45	3.41	2.7	2.7	4	8	1.2	1.1	3.45	3.40	2.7	2.6		0%
	Subcase <sub>12</sub> (medium)	4	1.1	3.45	4	1.1	3.45	4	6	1.1	1.0	3.45	2.8	2.8	2.4	4	6	1.1	1.0	3.45	2.91	2.9	2.8		3%
	Subcase <sub>13</sub> (large)	4	1.2	3.47	4	1.2	3.47	4	7	1.2	0.7	3.47	2.9	2.8	1.9	4	7	1.2	0.6	3.47	2.7	3.1	1.8		2.0%
Case II: FAULTS <sub>Sensor</sub>	Subcase <sub>21</sub> (small)	4	1.3	3.45	4	1.3	3.45	4	8	1.3	1.1	3.45	3.2	2.7	2.6	4	8	1.3	1.0	3.45	3.2	2.7	2.7		3.5%
	Subcase <sub>22</sub> (medium)	4	1.2	3.44	4	1.2	3.44	4	6	1.2	1.0	3.44	3.3	2.9	2.3	4	6	1.2	1.0	3.44	3.1	2.8	2.4		4%
	Subcase <sub>23</sub> (large)	4	1.1	3.46	4	1.1	3.46	4	7	1.1	0.6	3.46	2.8	3.1	2.0	4	6	1.1	0.7	3.46	2.7	2.8	1.9		6%
Case III: FAULTS <sub>Actuator</sub>	Subcase <sub>31</sub> (small)	4	1.1	3.45	4	1.1	3.45	4	8	1.1	0.8	3.45	3.2	2.8	2.6	4	8	1.1	0.8	3.45	3.2	2.8	2.6		2.5%
	Subcase <sub>32</sub> (medium)	4	1.2	3.44	4	1.2	3.44	4	6	1.2	0.4	3.44	3.1	3.1	2.8	4	6	1.2	0.4	3.44	3.3	3.1	2.3		5.5%
	Subcase <sub>33</sub> (large)	4	1.4	3.46	4	1.4	3.46	4	6	1.4	0.6	3.46	2.7	2.7	1.8	4	7	1.4	0.6	3.46	2.8	2.7	2.0		7%

TABLE III. ANALYSIS OF VARIOUS LEVELS OF LEAKAGE FAULTS, SENSOR FAULTS AND ACTUATOR FAULTS WITH FIXED AND ADAPTIVE MEWMA CONTROL CHART

EWMA Control Chart													
		Fixed Parameters			Variable Parameters								Improvement(%)
Cases	Subcase	Sample size n	Sampling Freq. h	UCL	n <sub>1</sub>	n <sub>2</sub>	h <sub>1</sub>	h <sub>2</sub>	UCL <sub>1</sub>	UCL <sub>2</sub>	w <sub>1</sub>	w <sub>2</sub>	Error detection
Case I: FAULTS <sub>Leakage</sub>	Subcase <sub>11</sub> (small)	3	1.1	10.44	3	7	1.1	0.4	10.44	10.44	2.7	2.3	3%
	Subcase <sub>12</sub> (medium)	3	1.2	10.44	3	9	1.2	0.6	10.44	10.44	2.9	2.5	3%
	Subcase <sub>13</sub> (large)	3	1.4	8.63	3	6	1.4	0.8	8.63	8.63	3.1	2.9	2%
Case II: FAULTS <sub>Sensor</sub>	Subcase <sub>21</sub> (small)	3	1.2	10.44	3	8	1.2	0.7	10.44	10.44	2.7	2.7	8%
	Subcase <sub>22</sub> (medium)	3	1.1	10.44	3	6	1.1	0.7	10.44	10.44	2.8	2.0	9%
	Subcase <sub>23</sub> (large)	3	1.2	10.44	3	6	1.2	0.7	10.44	10.44	2.8	2.3	11%
Case III: FAULTS <sub>Actuator</sub>	Subcase <sub>31</sub> (small)	3	1.3	10.44	3	9	1.3	0.8	10.44	10.44	2.8	2.1	11%
	Subcase <sub>32</sub> (medium)	3	1.2	10.44	3	6	1.2	0.4	10.44	10.44	3.1	1.9	12%
	Subcase <sub>33</sub> (large)	3	1.1	10.44	3	7	1.1	0.6	10.44	10.44	2.7	2.0	11%

TABLE IV. ANALYSIS OF VARIOUS LEVELS OF LEAKAGE FAULTS, SENSOR FAULTS AND ACTUATOR FAULTS WITH FIXED AND ADAPTIVE T<sup>2</sup> CONTROL CHART

T <sup>2</sup> Control Chart														
		Process Parameters												
		Fixed Parameters			Variable Parameters								Improvement(%)	
Cases	Subcase	Sample size n	Sampling Freq. h	UCL	n <sub>1</sub>	n <sub>2</sub>	h <sub>1</sub>	h <sub>2</sub>	UCL <sub>1</sub>	UCL <sub>2</sub>	w <sub>1</sub>	w <sub>2</sub>	Error detection	
Case I: FAULTS <sub>Leakage</sub>	Subcase <sub>12</sub> (small)	3	1.1	19.51	3	7	1.1	0.4	19.5	12.6	2.7	2.3	4%	
	Subcase <sub>13</sub> (medium)	3	1.2	13.66	3	9	1.2	0.6	13.6	14.6	2.9	2.7	2%	
	Subcase <sub>21</sub> (large)	3	1.4	17.6	3	6	1.4	0.8	17.6	14.8	3.1	2.6	6%	
Case II: FAULTS <sub>Sensor</sub>	Subcase <sub>22</sub> (small)	3	1.2	14.52	3	8	1.2	0.7	14.5	18.1	2.7	2.5	3.5%	
	Subcase <sub>23</sub> (medium)	3	1.1	15.5	3	6	1.1	0.7	15.5	14.1	2.8	2.5	5%	
	Subcase <sub>31</sub> (large)	3	1.2	13.7	3	6	1.2	0.7	13.7	13.8	2.8	2.4	6%	
Case III: FAULTS <sub>Actuator</sub>	Subcase <sub>31</sub> (small)	3	1.3	14.47	3	9	1.3	0.8	14.4	14.1	2.8	2.6	1.5%	
	Subcase <sub>32</sub> (medium)	3	1.2	15.1	3	6	1.2	0.4	15.1	13.8	3.1	2.2	11%	
	Subcase <sub>33</sub> (large)	3	1.1	13.8	3	7	1.1	0.6	13.8	14.6	2.7	1.6	11%	

